OPTIMIZING OF NEW APPROACH SINTERING METHOD ON CARBONATED HYDROXYAPATITE BIOCERAMIC

**Ahmad Fauzi Mohd Noor, Wai Yee Wong, Kee Chia Ching,
Zaw Linn Htun, and Radzali Othman**

School of Materials and Mineral Resources Engineering, Engineering Campus,
Universiti Sains Malaysia, Penang, Malaysia,
Tel: +60 604 599 6174, e-mail: srafauzi@usm.my

Abstract

Synthetic carbonated apatite ceramics are considered as alternative to autograft and allograft materials for bone substitute. This study was to investigate and compare the effect of carbonation introduced during cooling down of sintering of dense CHA with two kind of wet CO_2 atmosphere (direct wet CO_2 and dry CO_2 flow through water). Pelletized samples were sintered to 800°C and soaked for 120 minutes. Upon cooling down to 150, 200, 250 and 300°C, carbonation with wet CO_2 in desiccators were performed. The sintered CHA after carbonation at the various cooled temperatures was found to retain as B-type CHA. Carbonation of sintered CHA by dry CO_2 through water showed an overall better results as compared to carbonation by direct wet CO_2. Sample D200 with carbonation temperature of 200°C has the highest carbonate content (3.35%) and relative density (94%) while D250 with carbonation temperature of 250°C has the highest DTS value (18MPa). In vitro testing using SBF solution showed that apatite layer formed on the sintered CHA surface after one week of immersion, thus indicating the bone-forming ability. This indicated that the CHA synthesized in this study has sufficient biocompatibility to be applied as bone substitutes.

Keywords: Bioceramic, Carbonation, CHA, Mechanical properties, Sintering

Introduction

Hydroxyapatite (HA) has been used as biomaterial substitute for bone grafting since its chemical composition $Ca_{10}(PO_4)_6(OH)_2$ is similar to the inorganic component of the human bone[1,2]. However, its bioresorption rate is too slow to induce the formation of new bone. Lately however carbonated-substituted hydroxyapatite (CHA) are reported to be prospective as compared to HA as the chemical composition of the former CHA are much closely resemble the inorganic part of the bone tissue[2,3]. The carbonate content in bones varies from about 2 to 8 wt. % depending on the individual's age[3]. Although the carbonate ions in the bone mineral are small, it possesses a significant role in the biochemistry of hard tissue. Carbonate ions induce lower crystallite size and higher number of structural defects within the HA structure as well as reducing the sintering temperature to achieve high density body.

The carbonate ions can substitute at two sites in the hydroxyapatite structure, namely the hydroxyl and phosphate ion positions, which give rise to A-type and B-type of CHA[4]. The substitution can also occur simultaneously, resulting in AB-type of CHA

Typically, the amount of A-type or B-type is dependent on the age with the A/B ratio reported to be higher with the increase of human age. A-type CHA is found in old bone tissues while B-type CHA can be found in young bone tissues[5].

To densify and enhance the properties of CHA, sintering is typically an option. However, sintering causes decomposition of carbonate ions of CHA at high temperature. Chemically synthesized B-type CHA will decompose into HA and calcium oxide with CO_2 being released upon sintering at high temperature[6]. The loss of carbonate ions causes the formation of HA which have slow bioresorption rate. Poor control of the heat treatment of CHA results in the loss of carbonate ions consequently affecting the physical and mechanical properties.

Various different heat-treatment had been investigated in different gas atmospheres, including nitrogen, carbon dioxide, air, water vapor and wet oxygen. The gas atmosphere condition was reported to affect the decomposition significantly[6,7]. According to Landi et al. (2004)[7], thermal treatment in wet CO_2 gave the best result in terms of high carbonate residue with low A/B ratio in the range of the biological CHA.

Yanny and Ahmad-Fauzi (2011)[8] had investigated a new approach of sintering and carbonation of CHA. They found that the sintered samples achieved optimum densification sintering at 800°C by addition of sintering aids (magnesium hydroxide, $Mg(OH)_2$) while carbonation was performed at 200°C during cooling stage of sintering by using wet CO_2 had re-compensated the carbonate loss. In this current study, two different wet CO_2 atmospheres (i.e. direct wet CO_2 from tank and dry CO_2 flowing through water) were applied as carbonation during cooling period of sintering of CHA pellets. Since calcium is readily to react with CO_2 at a warm temperature during cooling, the main aim of the study is to compare the differences of final CHA properties of the samples sintered in these two carbonation atmospheres.

Experimental Procedure

The B-type CHA powder used in this study was synthesized by direct pouring technique via nanoemulsion route as reported by Zhou et al. (2008)[9]. The direct pouring route was found to be a relatively more effective technique than dropwise method (Kee et al., 2013)[10]. The molar ratio of the initial reagents of Ca^{2+}: PO_4^{3-}:CO_3^{2-} was set to be 1.67:1:1 and the synthesis was conducted in room temperature (25°C). The as-synthesized CHA powder was subsequently added with $Mg(OH)_2$, which plays the role as sintering aid. The mixed CHA+$Mg(OH)_2$ powders were later compacted at a pressure of 100 MPa and held constant for 120 seconds to ensure uniform pressure was applied on the pellets.

In this study, the compacted CHA pellets were sintered with a heating rate of 10°C/min to a temperature of 800°C and soaked for 120 minutes, and were subsequently cooled down at a rate of 10°C/min in a Lenton tube furnace. However, when the cooling temperature had reached 150°C, 200°C, 250°C or 300°C respectively, the pellets were quickly removed from the furnace and placed in a desiccator. Wet CO_2 gas direct from CO_2 tank was immediately flowed into the desiccator with a flow rate of 0.5L/min for 20 minutes. The samples were then left for 24 hours in the desiccator[8]. Another condition employed was the use of dry CO_2 which was flowed through water in a container bottle before flowing into the desiccator containing the warm sintered samples. The summary of samples codes of the sintered CHA pellets which were studied to indicate different

cooling atmosphere in which the pellets were removed from the furnace are shown in the Table 1.

The sintered CHA pellets were then characterized by X-ray diffraction (XRD), Fourier transform infrared (FTIR), field emission scanning electron microscope (FESEM), Carbon, Hydrogen and Nitrogen (CHN) analyzer, bulk density and porosity measurement, diametral tensile strength (DTS) and the bioactivity evaluation of the pellets by simulated body fluid (SBF).

Table 1. Sample Codes of Sintered CHA Pellets of Different Cooling Atmosphere and Different Temperature Evacuated from Furnace

| Carbonation Condition	Temperature at which Samples Removed from Furnace (°C)			
	150	200	250	300
Wet Direct CO_2	W150	W200	W250	W300
Dry CO_2 Through Water	D150	D200	D250	D300

Results and Discussion

XRD Analysis

Figure 1 (a) and (b) shows the XRD spectra of the sintered CHA pellets treated with the different carbonation at four different cooling temperatures after sintering. It can be analyzed that all the peaks shown in Figure 1 (a) and (b) match with the reference XRD pattern of HA (ICDD: 00-009-0432) and had the same XRD peak positions. The same samples were all sintered to same temperature (800°C) with difference being the carbonation temperature and carbonation condition. The diffraction peaks includes $2\Theta = 25.77°$ (002), $2\Theta = 28.02°$ (102), $2\Theta = 28.87°$ (210), $2\Theta = 34.04°$ (202), $2\Theta = 39.94°$ (310), $2\Theta = 43.86°$ (113), $2\Theta = 46.71°$ (222), $2\Theta = 41.45°$ (213) and $2\Theta = 53.10°$ (004) which was the major peaks of HA. The used of HA as reference would allow the analysis to determine if the sintered samples are A-type, B-type or AB-type CH, based on the c/a ratio.
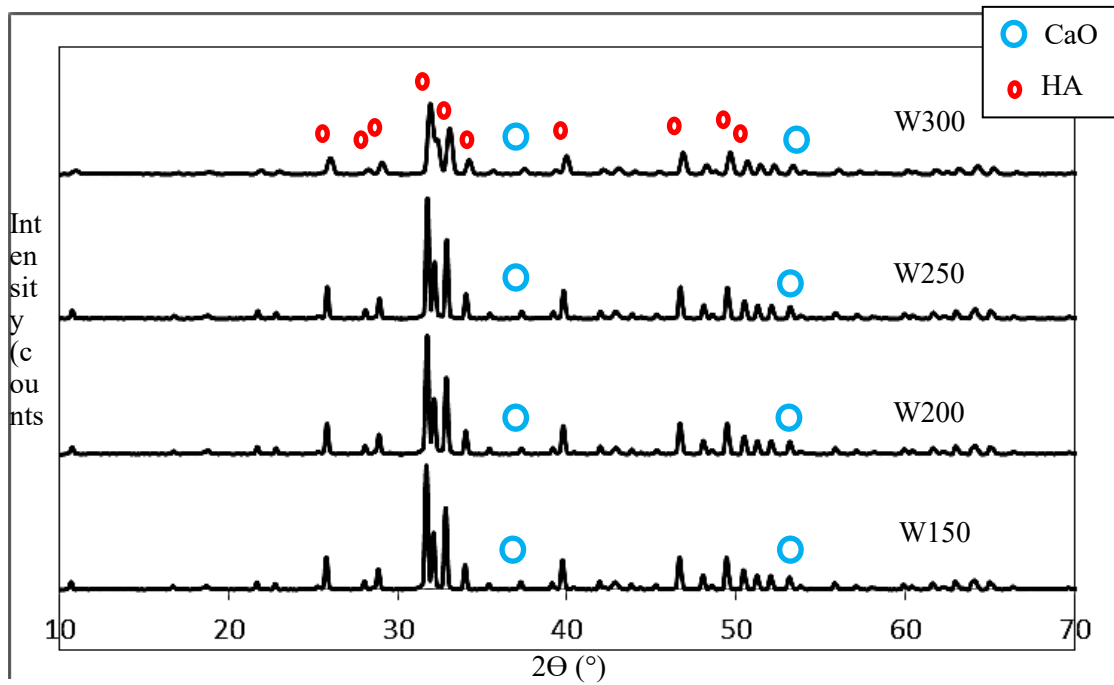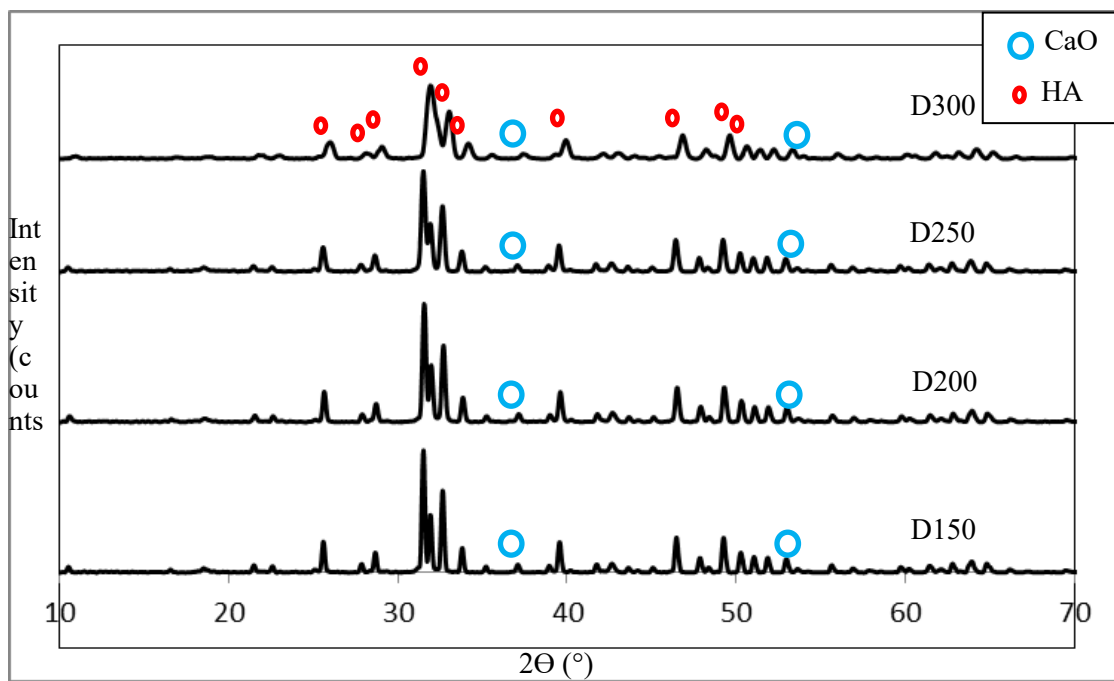
Figure 1. XRD spectrum of carbonation by (a) direct wet CO_2 and (b) dry CO_2 through water

Sintering of CHA at 800°C had resulted in the partial decomposition of CHA. This is indicated with the presence of peaks corresponding to secondary phase of CaO as shown in Figure 4.6(a) and (b) at $2\Theta = 37.20°$ and $53.70°$.

**Table 2. Lattice Parameters, *c/a* Ratio and Crystallite Size of Sintered CHA Treated with Wet Co_2**

Condition	Sample	a-axis, (Å)	c-axis, (Å)	c/a	Crystallite Size, (nm)
Direct wet CO_2	W150	9.4144	6.8775	0.7305	123.2
	W200	9.4168	6.8799	0.7306	100.76
	W250	9.4166	6.8797	0.7306	125.11
	W300	9.4206	6.8832	0.7307	31.11
Dry CO_2 through water	D150	9.4109	6.8749	0.7305	98.93
	D200	9.4129	6.8768	0.7306	58.80
	D250	9.4154	6.8788	0.7306	44.85
	D300	9.4188	6.8819	0.7307	23.01

The results shown in Table 2 suggest that the samples W150-W300 had crystallite size generally larger than D150-D300. This shows that the condition of carbonation had effect on the crystallite size of the CHA. Using wet CO_2 directly from CO_2 tank onto the cooled sintered CHA after cooling had produced larger crystallite size, as compared to carbonation by CO_2 flowing through water. It can also be seen from Table 2 that increasing the carbonation temperature during cooling (*i.e.* cooling temperature after sintering) also affects the crystallite size with higher carbonation temperature showing reduced crystallite size.

Carbonate ion substitution has been reported also to have the effect of inducing lower crystallite size of the HA structure[3]. Generally, it can be predicted that the carbonate content in D150-D300 are higher than W150-W300 and the grain size of W150-W300 are larger than D150-D300 based on the results of crystallite size.
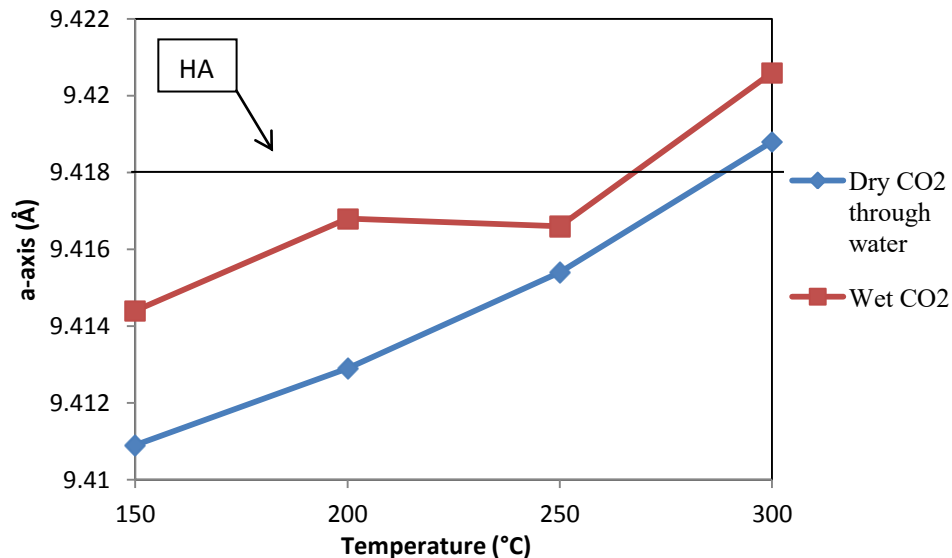
(i)
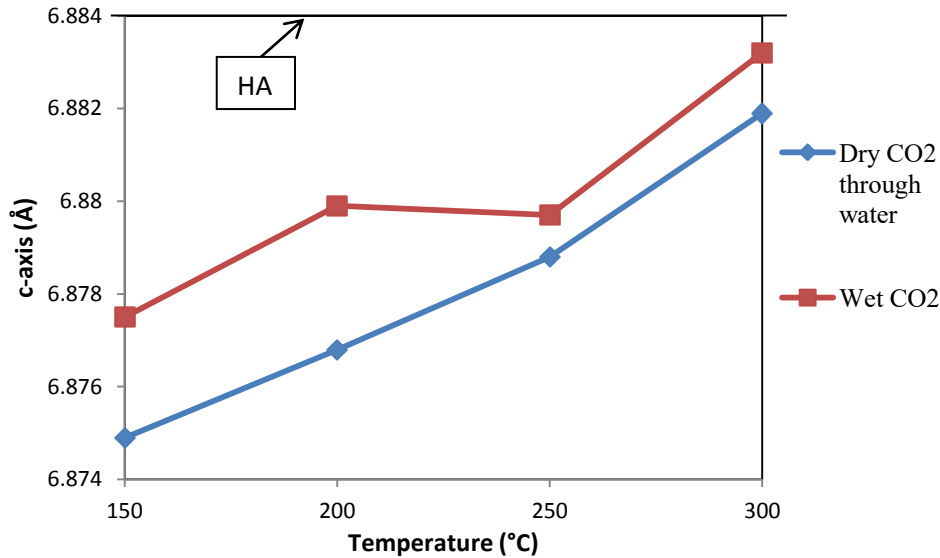
(ii)

Figure 2. Trend of (i) *a*-axis and (ii) *c*-axis on the carbonation temperature by two different CO_2 atmospheres (note: HA is reference data)

From Figure 2, the lattice parameters of *a*-and *c*-axis show the trend of small increase with the increasing carbonation temperature. According to Landi et al, (2004)[7], A-type substitution of carbonate in HA structure will result in extension of *a*-axis and contraction of *c*-axis while B-type substitution of carbonate will results in contraction of *a*-axis and extension of *c*-axis. Figure 2 shows the contraction of *a*-and *c*-axis. This results was also shown similarly by Tkachenko and Zyman (2008)[11] in the sintering of CHA at 800°C. It is difficult to predict the nature of alteration based solely on XRD results, hence FTIR characterization was subsequently taken into consideration.

FTIR Analysis

Figure 3 shows the FTIR spectra of synthesized CHA powder and sintered CHA pellets treated with direct wet CO_2 from the Co2-gas tank and dry CO_2 through water. Bands corresponding to phosphate group were detected at 472, 568, 958, and 1020-1120 cm^{-1}. The presence of water in synthesized CHA powder (bands at 1636 and 3437 cm^{-1}) were not detected in the sintered CHA pellets, thus suggesting that the moisture was removed after sintering.

Samples W150-W300 and D150-D300 has similar peak position in FTIR spectra. The typical stretching bands of OH^- at 630 and 3570 cm^{-1} were detected in the sintered CHA pellets, but were not traced in synthesized CHA powder. This shows that sintered CHA pellets treated by the two kind of wet CO_2 condition had re-compensated the carbonate at PO_4^{3-} side, which results in B-type CHA being retained after the sintering and new approach carbonation schedules.

The typical stretching bands of B-type CHA at 870-875, 1410-1430 and 1450-1470 cm^{-1} were detected in all sintered CHA. There was no A-type CHA stretching bands (at 877-880, 1500 and 1540-1550 cm^{-1}) detected. This clearly indicated that the sintered CHA pellets upon cooling in the different carbonation condition were B-type CHA.
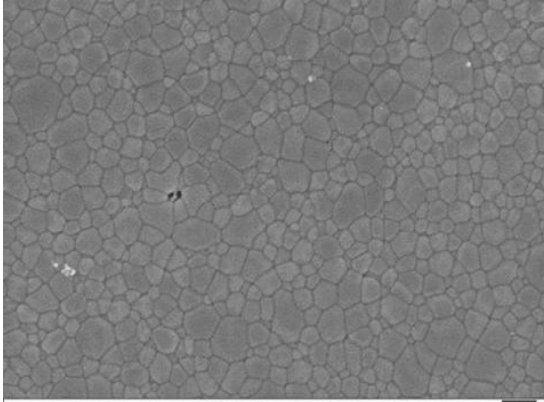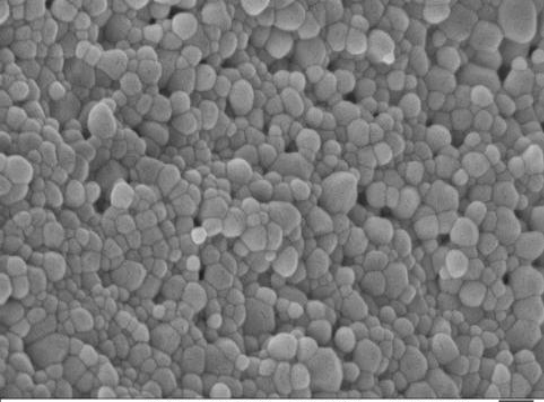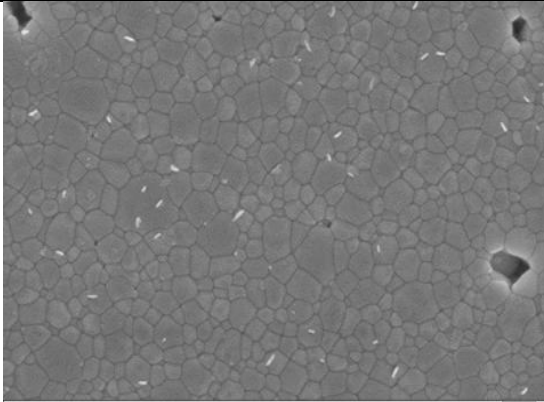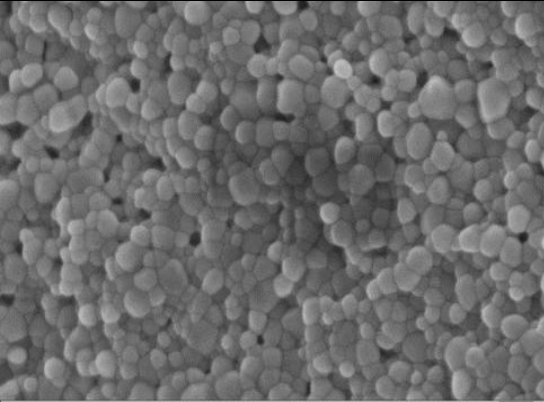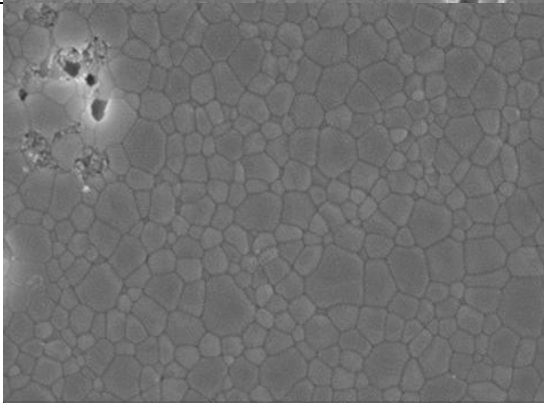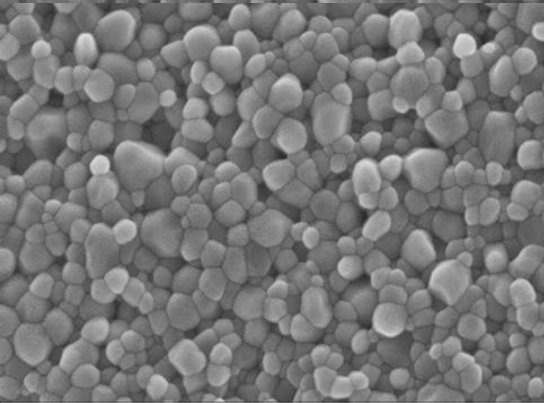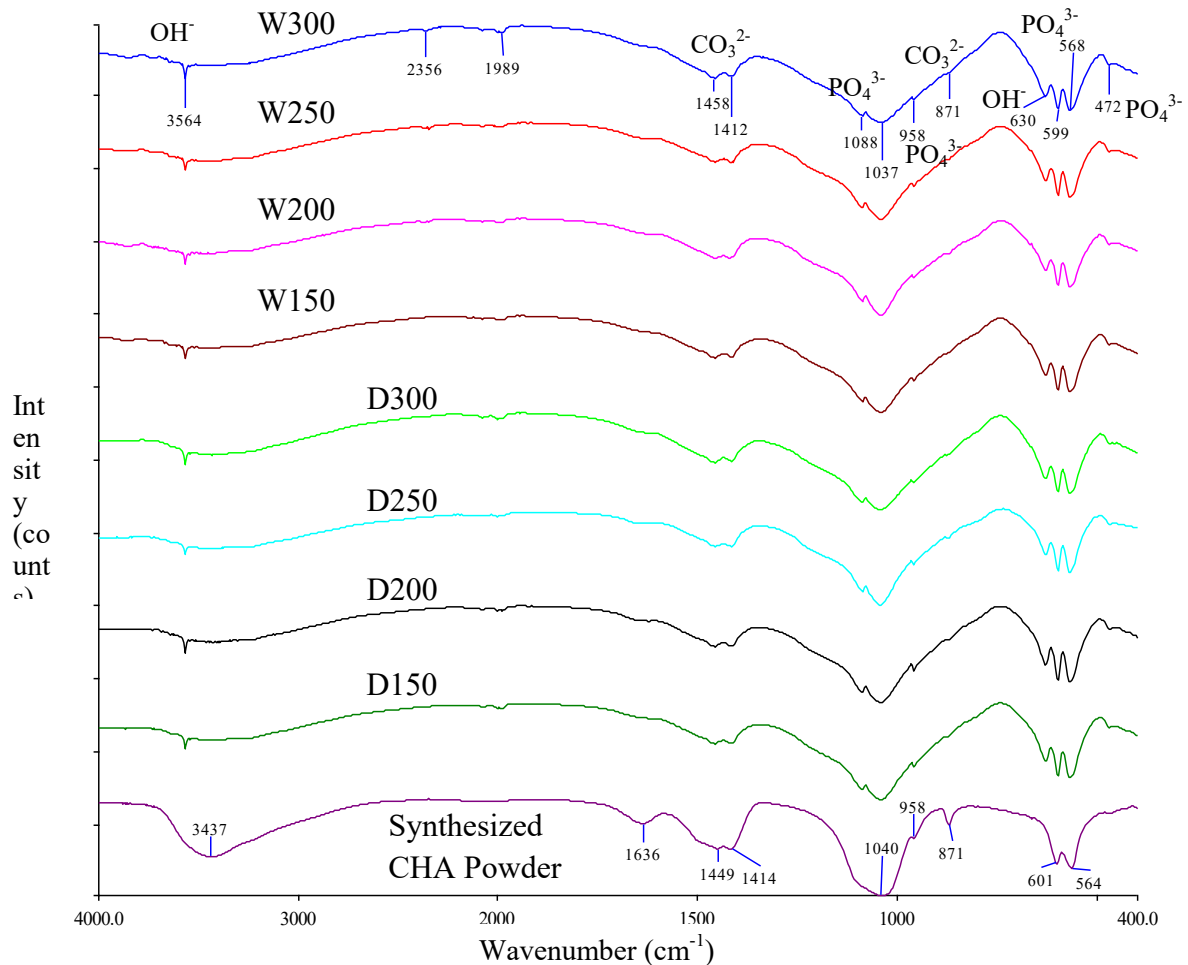

Figure 3. FTIR spectra of synthesized CHA powder and sintered CHA pellets carbonated with wet CO_2 and dry CO_2 through water

Microstructural Study Using FESEM

The various CHA pellets were thermally etched at 700 °C for 30 minutes to reveal the microstructure before the observation with FESEM. Figure 4 shows the microstructure of the top surface and the fracture surface of CHA pellets treated with direct wet CO_2. The estimated grain size is shown in Table 3. It can be seen that the sintered pellets were densified, with minimal pore formation. The sintering temperature of 800 °C had sufficiently densified the sintered pellet. The density and porosity will be discussed later.

| Sample	Top Surface	Facture Surface
W150	Mag = 30.00 K X 200 nm' WD = 5.1 mm EHT = 5.00 kV Signal A = InLens Date :8 Apr 2013 Time :21:16:51	Mag = 30.00 K X 200 nm' WD = 5.1 mm EHT = 5.00 kV Signal A = InLens Date :8 Apr 2013 Time :21:35:01
W200	Mag = 30.00 K X 200 nm' WD = 5.0 mm EHT = 5.00 kV Signal A = InLens Date :8 Apr 2013 Time :21:07:23	Mag = 30.00 K X 200 nm' WD = 5.0 mm EHT = 5.00 kV Signal A = InLens Date :8 Apr 2013 Time :21:05:28
W250	Mag = 30.00 K X 200 nm' WD = 5.1 mm EHT = 5.00 kV Signal A = InLens Date :8 Apr 2013 Time :21:39:03	Mag = 30.00 K X 200 nm' WD = 5.1 mm EHT = 5.00 kV Signal A = InLens Date :8 Apr 2013 Time :21:19:03

| W300 | | |
| D200 | | |
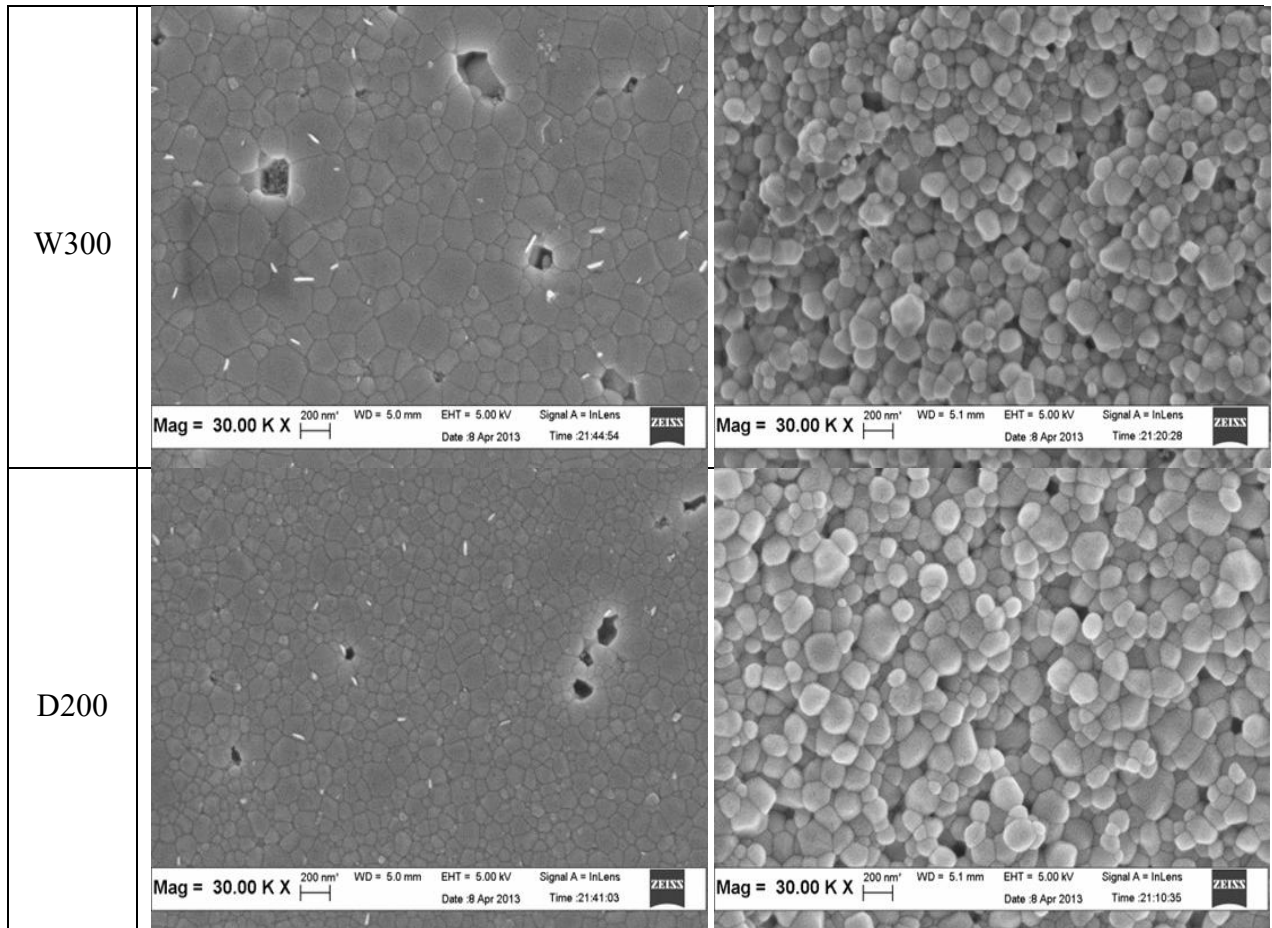
Figure 4. FESEM images of CHA pellet surfaces and facture surfaces treated with direct wet CO_2 (150°C, 200°C, 250°C and 300°C) and dry CO_2 that flow through water (200°C)

Generally, the surface microstructure in Figure 4 and the estimated grain size (Table 3) shows that W300 (165 nm) has coarser grains followed by W250 (154nm), W200 (134) and W150 (132nm). It was also observed that the grain size of W150 and W200 were more homogeneous compared to the higher W250 and W300. This clearly shows that higher carbonation temperature produced larger grain size in CHA and promotes abnormal grain growth (rapid growth of a few larger grains at the expense of the smaller grains) during the densification process. However, grains observed on the fracture surfaces showed little difference among the different carbonation temperatures as compared to the microstructure at the surfaces. This can be attributed to the carbonate substitution being more readily on the CHA pellets surface during carbonation, as compared to those in the middle section of the pellets.

Table 3. Estimated Grain Size of CHA Pellets Treated with Different CO_2 at Different Temperatures

Sample	W150	W200	W250	W300	D200
Estimated grain size (nm)	132	137	154	165	93

From images of top surface in Figure 4, it can be observed that W300 have the largest pores size when compared to the W150, W200 and W250. The pores were isolated and located at the grain boundaries. This would be explained as a result of the liquid phase sintering by using $Mg(OH)_2$ as sintering aid[8]. The low porosity was due to treatment with wet CO_2 had promote densification and inhibit abnormal grain growth.

The D200 sample which was sintered at $800^{o}C$ and treated with dry CO_2 that flow through water showed the smaller grain (93 nm) as compared to the ones by wet CO_2 (137 nm). This indicated that samples treated by dry CO_2 flowing through water would inhibit grain growth as compared to direct wet CO_2 from gas tank. In addition, the pores were also observed to be situated at the grain boundaries.

CHN Analysis of Sintered Samples

Before sintering, the carbonate content of as-synthesized CHA determined by CHN was 8.25%. After sintering, the carbonate content of the sintered samples treated with different condition of CO_2 is shown in Table 4. Based on the results, there was reduction of carbonate content after sintering. However all the carbonate content in the sintered CHA was in the range of 2 - 3.5%. The amount of carbonate content retained in the CHA is within the range required in human bone. In this work, the carbonation procedure was intended to re-compensate the carbonate loss during sintering.

The introduction of dry CO_2 passing through water during cooling stage of sintering of CHA have overall highest level of carbonate content. This shows that using dry CO_2 flowing through water will re-compensate more carbonate ions to the CHA lattice upon sintering as compared to the direct flow wet CO_2 from CO_2 gas tank.

Table 4. Carbon and Carbonate Content of Sintered CHA Treated by Different Condition of CO_2

CO_2 Condition	Sample	C Content (%)	Carbonate Content (%)	Carbonate Loss (%)
Wet CO_2	W150	0.53	2.65	68
	W200	0.56	2.80	66
	W250	0.60	3.00	64
	W300	0.53	2.65	68
Dry CO_2 trough water	D150	0.56	2.80	66
	D200	0.67	3.35	59
	D250	0.64	3.20	61
	D300	0.53	2.65	68

Relative Density and Porosity Measurements

Density and porosity measurements of the various sintered CHA pellet were also performed using Archimedes Principles while the true density of the CHA powder was obtained by gas pycnometer. The powder density of CHA was 2.868 g/m^3. The comparison of the relative density of sintered CHA is shown in Figure 5. It can be observed that the various sintered CHA pellets have high relative density, which is in the range of 87.9% to 93.9%. This shows that the addition of $Mg(OH)_2$ as sintering aid to the nano-structured CHA had assisted the sintering process at a low temperature of 800°C to achieve high densification.
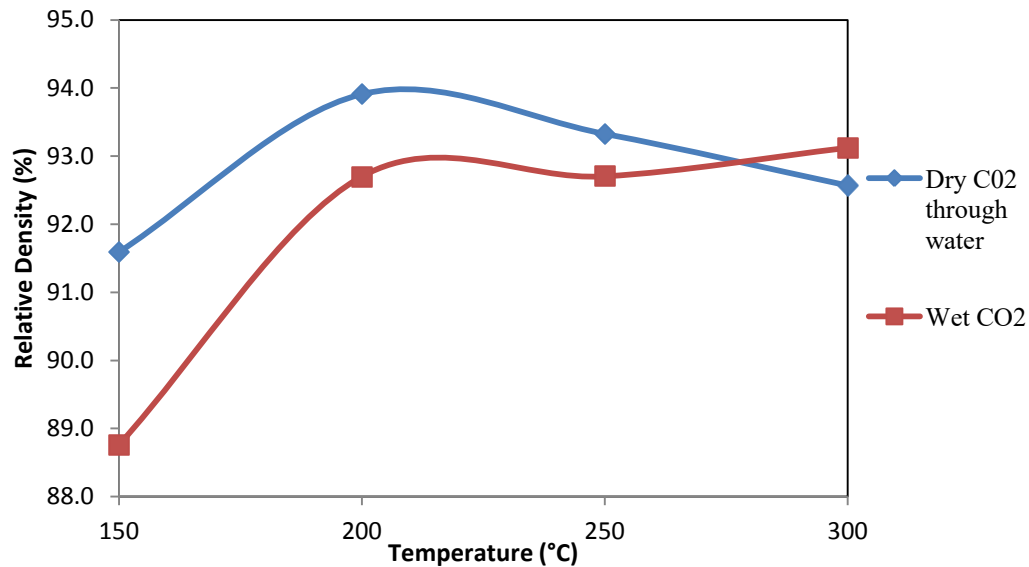

Figure 5. Graph of relative density of sintered CHA treated with different CO_2 at different temperature

It can also be reported that sintered CHA pellets treated with dry CO_2 through water have an overall higher relative density when compared to direct wet CO_2 during carbonation process. The effect of wet CO_2 was associated with the shrinkage acceleration during compact densification, where the particles would slide into the voids and pores between them[11]. Sample D200 had the highest relative density than other samples. From the CHN analysis, D200 has the highest carbonate content from the CHN analysis. The presence of wet CO_2 not only helped in compensating carbonate loss during sintering, it also assisted in densification of the sintered samples.

Diametral Tensile Strength (DTS)

DTS was done to obtain the ultimate compressive strength of the sintered CHA pellets (Figure 6). Among the sintered CHA pellets treated with wet CO_2, W200 has the highest DTS value (14 MPa) while the samples treated with dry CO_2 through water, D250 has the highest DTS value (18 MPa).
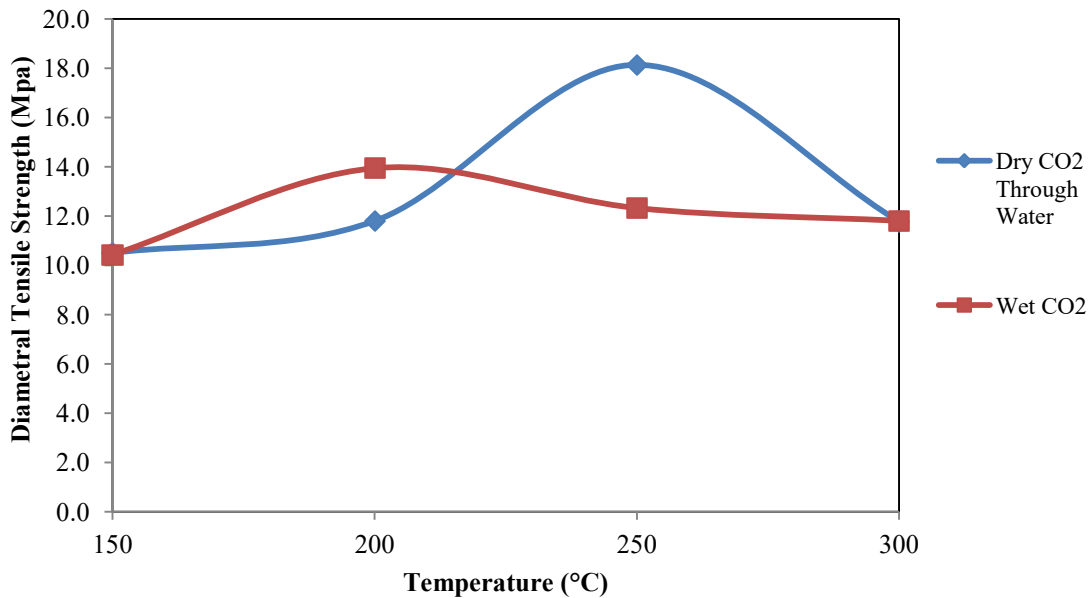
Figure 6. DTS results of sintered CHA pellets treated with different CO_2 atmospheres at different temperature

From Figure 6, carbonation by wet CO_2 produced sintered CHA pellets with small range of DTS value. Carbonation by dry CO_2 through water on the other hand had the highest DTS value at carbonation temperature of 200°C. Referring to the SEM images in Figure 4, carbonation by dry CO_2 through water has small grain size. Smaller size of grains has more grain boundaries, and thus showing higher strength[12].

From the results obtained, the DTS value of D250 (18 MPa) was higher than the compressive strength of trabecular bone (2-12 MPa). However, it was lower than the compressive strength of cortical bone (100-230 MPa), thus suggesting that it has potential use for non-load bearing application.

Biological Evaluation SBF of Sintered CHA

Biological evaluation of the sintered CHA pellets was conducted by immersing the samples in the Simulated Body Fluid (SBF) at 36.5°C. SBF is a synthetic solution with an ionic content and concentration comparable to human plasma[13]. The SBF was prepared according to the method by Kokubu et al. (2006)[14]. The samples chosen to be biologically evaluated in this study were W200, D200 and D250. These samples were selected as they showed the highest carbonate content (D200) and highest ultimate tensile strength (D250 and W200). Figure 7 shows the SEM images of W200 after the immersion in SBF solution for one, two and four weeks, while Figure 8 shows the SEM images of D200 and D250 after the immersion in SBF solution for one week.
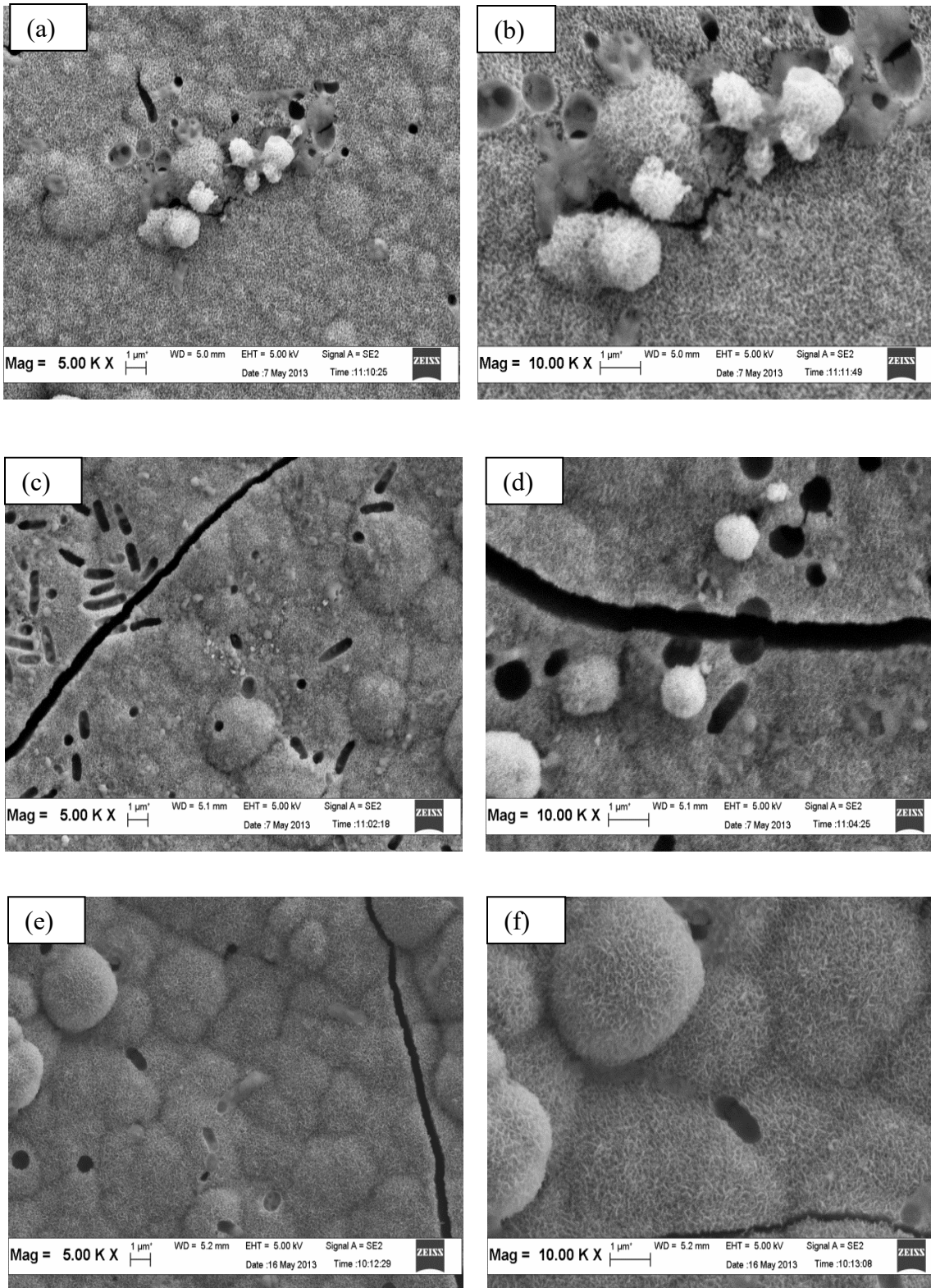
Figure 7. FESEM images of W200 immersed in SBF for 1 week (a) & (b), 2 weeks (c) & (d) and 4 weeks (e) & (f)

It was observed that the apatite layer had formed on the CHA pellets of W200 surface after one week of immersion in SBF (Figure 7). It was also reported by Gibson et al. (2002)[13] that apatite layer was formed on CHA after seven days of immersion in SBF. The apatite layer was porous in structure. After two weeks of immersion, the structure of apatite layer became denser. At four week of immersion, the apatite layer became more dense and homogeneous.
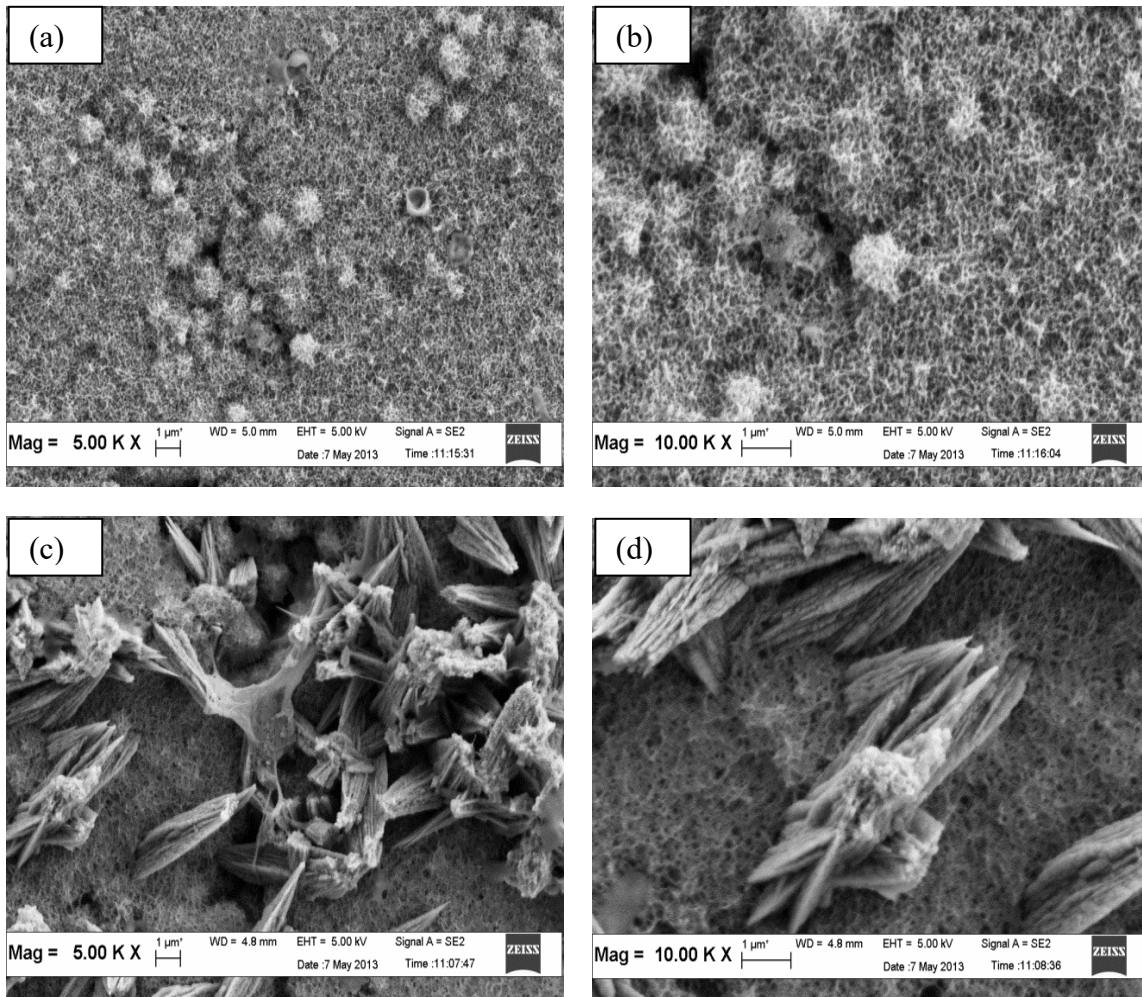

Figure 8. FESEM images of D200 (a) & (b) and D250 (c) & (d) immersed in SBF for one week

From Figure 8 (a) and (b), the apatite layer in porous structure was formed on the surface of the D200 at the first week of immersion in SBF. As compared to W200, it can be seen that the apatite crystal (needle-shape) are coarser and well-spread. This indicates D200 sample is more active in formation of apatite layer, being more bioactive. The apatite layers of D250 in Figure 8 (c) and (d) were in rosette structure which were coarser as compare to W200 and D200. The biological evaluation shows that the CHA samples produced in this study employing new approach of carbonation were bioactive since the apatite was able to form after one week of immersion in SBF.

Conclusions

In conclusion, the new approached of sintering of CHA with carbonation introduced during cooling stage of this study had resulted in the retention of B-type CHA with carbonate content in the range of 2 to 3.5%. Carbonation using dry CO2 flowing through container of water had shown better physical and mechanical properties with improved bioactivity indicated with rapid formation of apatite when immersed in SBF. The CO2 introduced during cooling stage after sintering was to recompensate the carbonate loss and cooling temperature of 200 to 250°C was most effective with smaller grain size and thus improved mechanical properties. The addition of Mg(OH)2 as sintering aid had enabled sintering of nano-sized CHA to be performed at a low temperate of 800°C , thus minimizing loss of carbonate during sintering.

Acknowledgement

References

[1] M.P. Ferraz, M.H. Fernandes, A.T. Cabral, J.D. Santos, and F.J. Monteiro, "In vitro growth and differentiation of osteoblast-like human bone marrow cells on glass reinforced hydroxyapatite plasma-sprayed coatings," *Journal of Materials Science: Materials in Medicine*, Vol. 10, No. 9, pp. 567-576, 1999.

[2] Y.Y. Filippov, E.S. Klimashina, A.B. Ankudinov, and V.I. Putlayev, "Carbonate substituted hydroxyapatite (CHA) powder consolidated at 450°C," *Journal of Physics: Conference Series*, Vol. 291, No. 1, 2011.

[3] A. Porter, N. Patel, R. Brooks, S. Best, N. Rushton, and W. Bonfield, "Effect of carbonate substitution on the ultrastructural characteristics of hydroxyapatite implants," *Journal of Materials Science: Materials in Medicine,* Vol. 16, No. 10, pp. 899-907, 2005.

[4] S.M. Barinov, J.V. Rau, S.N. Cesaro, J. Ďurišin, I.V. Fadeeva, D. Ferro, L. Medvecky, and G. Trionfetti, "Carbonate release from carbonated hydroxyapatite in the wide temperature rage," *Journal of Materials Science: Materials in Medicine,* Vol. 17, No. 7, pp. 596-604, 2006.

[5] E. Landi, G. Celotti, G. Logroscino, and A. Tampieri, "Carbonated hydroxyapatite as bone substitute," *Journal of the European Ceramic Society,* Vol. 23, No. 15, pp. 2931-2937, 2003.

[6] J.E. Barralet, S.M. Best, and W. Bonfield, "Effect of sintering parameters on the density and microstructure of carbonate hydroxyapatite," *Journal of Materials Science: Materials in Medicine,* Vol. 11, No. 11, pp. 719-724, 2000.

[7] E. Landi, A. Tampieri, G. Celotti, L. Vichi, and M. Sandri, "Influence of synthesis and sintering parameters on the characteristics of carbonate apatite," *Biomaterials,* Vol.25, No. 10, pp. 1763–1770, 2004.

[8] Y.M.B. Ismail, and A.F.M. Noor, "Effect of a novel approach of sintering on physical properties of carbonated hydroxyapatite," *Journal of Materials Science and Engineering B,* Vol. 1, pp. 157-163, 2011.

[9] W.Y. Zhou, M. Wang, W.L. Cheung, B.C. Guo, and D.M. Jia, "Synthesis of carbonated hydroxyapatite nanospheres through nanoemulsion," *Journal of Materials Science: Materials in Medicine,* Vol. 19, No. 1, pp. 103–110, 2008.

[10] C.C. Kee, H. Ismail, and A.F.M. Noor, "Effect of synthesis technique and carbonate content on the crystallinity and morphology of carbonated hydroxyapatite," *Journal of Materials Science & Technology,* Vol. 29, No. 8, pp. 761-764, 2013.

[11] M.V. Tkachenko, and Z.Z. Zyman, "Effect of sintering conditions on physical properties of carbonated hydroxyapatite ceramics," *Functional Materials,* Vol. 15, No. 4, pp. 574-578, 2008.

[12] S. Ramesh, C. Tan, S. Bhaduri, and W. Teng, "Rapid densification of nanocrystalline hydroxyapatite for biomedical applications," *Ceramics International,* Vol. 33, No. 7, pp. 1363-1367, 2007.

[13] I.R. Gibson, and W. Bonfield, "Novel synthesis and characterization of an AB-type carbonate-substituted hydroxyapatite," *Journal of Biomedical Materials Research,* Vol. 59, No. 4, pp. 697-708, 2002.

[14] T. Kokubo, and H. Takadama, "How useful is SBF in predicting in vivo bone bioactivity?," *Biomaterials,* Vol. 27, No. 15, pp. 2907-2915, 2006.